Kinetic Transition Networks for the Thomson Problem and Smale's 7th Problem

Dhagash Mehta,[1, 2, *] Jianxu Chen,[3, †] Danny Z. Chen,[3, ‡] Halim Kusumaatmaja,[4, §] and David J. Wales[5, ¶]

[1]*Department of Applied and Computational Mathematics and Statistics,*
University of Notre Dame, Notre Dame, IN 46556, USA.
[2]*Centre for the Subatomic Structure of Matter, Department of Physics,*
School of Physical Sciences, University of Adelaide, Adelaide, South Australia 5005, Australia.
[3]*Department of Computer Science and Engineering,*
University of Notre Dame, Notre Dame, IN 46556, USA.
[4]*Department of Physics, Durham University, South Road, Durham DH1 3LE, United Kingdom.*
[5]*University Chemical Laboratories, Lensfield Road, Cambridge CB2 1EW, United Kingdom.*

The Thomson Problem, arrangement of identical charges on the surface of a sphere, has found many applications in physics, chemistry and biology. Here we show that the energy landscape of the Thomson Problem for N particles with $N = 132, 135, 138, 141, 144, 147,$ and 150 is single funnelled, characteristic of a structure-seeking organisation where the global minimum is easily accessible. Algorithmically constructing starting points close to the global minimum of such a potential with spherical constraints is one of Smale's 18 unsolved problems in mathematics for the 21st century because it is important in the solution of univariate and bivariate random polynomial equations. By analysing the kinetic transition networks, we show that a randomly chosen minimum is in fact always 'close' to the global minimum in terms of the number of transition states that separate them, a characteristic of small world networks.

INTRODUCTION

The Thomson Problem is an important model in both physics and chemistry and is easily stated: find the minimum energy of a system composed of N identical charges that are constrained to move on the surface of a sphere of unit radius, i.e. minimise the potential energy function

$$V_{\text{Th}}(\mathbf{r}) = \sum_{1 \leq i < j \leq N} \frac{1}{r_{ij}}, \qquad (1)$$

where $r_{ij} = \sqrt{(x_i - x_j)^2 + (y_i - y_j)^2 + (z_i - z_j)^2}$, subject to spherical constraints $x_i^2 + y_i^2 + z_i^2 = 1$ for all $i = 1, \ldots, N$.

The model was proposed by J. J. Thomson as a representation of atomic structure [1], although it was soon abandoned in this context. However, it has subsequently found many applications in physics, chemistry and biophysics because it captures the competition between local order for neighbouring particles and long-range constraints due to the curvature and geometry. In particular, it is not generally possible to arrange every particle in an identical environment. The resulting model can provide insight into the forces governing far more complex systems, such as the arrangement of proteins in shells of spherical viruses [2–5], fullerene patterns for carbon clusters [6], the surface ordering of liquid metal drops confined in Pauli traps [7], and the behaviour of colloidal particles trapped at a fluid-fluid interface [8–15].

In the mathematics and computer science communities, the Thomson Problem has gained special attention because it appears in the 7th problem in Steven Smale's list of eighteen unsolved problems for the 21st century [16, 17]. The problem as posed by Smale [18] requires us to algorithmically construct a collection of starting points [19] say $\mathbf{r}^*$, so that for a given number of particles N, $V_{\text{Th}}(\mathbf{r}^*) - V_{\text{Th}}(\mathbf{r}_{\text{gm}}) \leq \text{const} \times \log N$, for $N \geq 2$. Here, $\mathbf{r}_{\text{gm}}$ is the global minimum for the given N.

Constructing such points corresponds to finding a good starting system of polynomial equations to locate all the complex solutions for sets of polynomial equations and to realise the Fundamental Theorem of Algebra [20]. Recently, another interesting development came from Armentano-Beltrán-Shub for a logarithmic version of the potential [21]: one first finds all the N complex roots of the N-degree random univariate polynomial equation with the Kostlan formulation [22], i.e., $\sum_{i=0}^{N} a_i x^i = 0$, where the complex numbers a_i are independently drawn from the Gaussian distribution with mean 0 and variance $\binom{N}{i}$, for all $i = 0, \ldots, N$. This formulation of the random univariate polynomial equation is different than the original Kac formulation [22] in which the complex numbers are independently drawn from the Gaussian distribution with mean 0 and variance 1. Then, from these N roots, using a steregraphic mapping as prescribed in [21], one obtains 2 real numbers per root, corresponding to coordinates on the 2-sphere. Armentano-Beltrán-Shub showed that, in the probabilistic sense, the set of these N coordinates is a reasonable choice (if not strictly $\log N$ close) for the initial points for the global minima of the Thomson Problem with N particles.

Given its broad relevance, the global minimum of the Thomson Problem has been studied extensively [23–36]. Analytical solutions are known for $N = 2 - 6$ and 12 [37, 38]. For $N = 4, 6$ and 12, they correspond to Platonic solids. The global minimum structures for larger N have been tackled computationally [31, 32, 39–47]. Most of these studies, however, only focus on the global minima. In the present work we search extensively for (most, if not all) the minima and transition states of the Thomson Problem at some selected sizes up to $N = 150$, and study the networks defined by these minima and the transition states that connect them. Using disconnectivity graphs [48, 49], we find that the Thomson Problem exhibits a single funnel for all N considered. We also show that the networks exhibit typical characteristics of a small world network. Ihence, in the context of Smale's 7th problem, all minima are only a few

steps from the global minimum.

POTENTIAL ENERGY LANDSCAPES OF THE THOMSON PROBLEM

We begin by collecting some basic definitions: a local minimum of a potential is a point in the configuration space where the gradient vanishes and at which the Hessian matrix has no negative eigenvalues. The minimum at which the potential attains the lowest value is the global minimum. A transition state [50] is a configuration where the gradient vanishes, and exactly one eigenvalue of the Hessian matrix is negative. Transition states define connections between pairs of minima via steepest-descent paths. Hence, we can construct kinetic transition networks [51–53] of local minima and the transition states that link them for a given potential.

To perform an extensive search for local minima and transition states of the Thomson Problem, we employed the GMIN [54] and OPTIM programs [55]. To identify likely global minima we applied basin-hopping global optimisation [56–59]. In this method, random geometrical perturbations are followed by energy minimisation, and moves are accepted or rejected based upon the energy differences between local minima. This procedure transforms the energy landscape system into the set of catchment basins for the local minima. For all the minimisations in the present work a modified version of the limited-memory Broyden–Fletcher–Goldfarb–Shanno (LBFGS) algorithm [60, 61] was used. This scheme has proved to be the most efficient in recent benchmarks [62].

We used a combination of the doubly-nudged elastic band (DNEB) and hybrid eigenvector-following techniques to find the transition states [63]. In DNEB, a series of images interpolate between the two end points, and the total energy is minimised subject to spring constraints between adjacent images. Maxima in the DNEB path are then adopted as transition state candidates, which we refine to high precision using hybrid eigenvector-following [64–66]. Here we use a Rayleigh-Ritz approach [59] to compute the smallest non-zero eigenvalue, and take an uphill step along the corresponding eigendirection. We then minimize in the tangent space for a limited number of steps, so that the gradient does not develop a significant component in the uphill direction. We project out all components corresponding to zero Hessian eigenvalues. For the Thomson Problem these are the three modes associated with overall rotations around the x, y, and z axes. Using spherical polar coordinates (ϕ, θ), the corresponding eigenvectors are

$$\hat{e}_x = (\cos\theta\cos\phi/\sin\theta, \sin\phi)$$
$$\hat{e}_y = (-\cos\theta\sin\phi/\sin\theta, \cos\phi) \qquad (2)$$
$$\hat{e}_z = (1, 0).$$

For each transition state we applied small displacements in the two downhill directions and minimised the energy to identify minimum-transition state-minimum triplets. In some cases, new local minima may be identified in this pro-
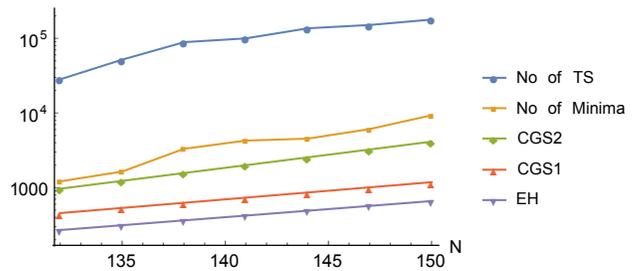

Figure 1: 'TS' refers to 'Energetically Distinct Transition Sates', 'EH' refers to the estimate of the number of minima given in [26], 'CGS1' is a recent [68] fit to the number of minima found in previous calculations, and 'CGS2' is an estimate [68] for the number of minima (we use the maximum out of those suggested in [68].) The lines connecting data points are a guide to the eye.

cedure. By iterating the process, we systematically build a connected database of stationary points.

Our results for the number of minima and transition states at $N = 132, 135, 138, 141, 144, 147$ and 150 are shown in Figure 1. In all cases [67] we have obtained more minima than previous results given in the literature [26, 68]. It is known that usually the number of local minima for a molecular system increases exponentially with system size [26, 69, 70]. This scaling applies here, and locating likely candidates for the global minimum becomes increasingly difficult for larger systems. However, the rate of increase is relatively slow for the Thomson Problem, because the Coulomb potential is long-ranged [71–73].

Disconnectivity graphs provide a powerful way to visualize the organization of minima and transition states [48, 49]. A disconnectivity graph is a tree graph where the vertical axis corresponds to the potential energy. Each line terminates at the energy of a local minimum, and the minima are joined at the lowest energy where they can interconvert for regularly spaced energy thresholds. These connections are defined by the highest transition state on the lowest energy path between each pair of minima.

The disconnectivity graph for the databases considered here is shown in Figure 2 for $N = 147$. It shows a typical structure-seeking 'palm tree' organisation [49], where there is only a single funnel in the potential energy landscape and the energy barriers separating local energy minima and the global minimum are small. The same qualitative features are observed for all particle numbers we have considered, up to $N = 150$. This organisation is associated with efficient relaxation to the global minimum.

NETWORK PROPERTIES

For each N, we construct a network G in which each node corresponds to a unique minimum energy structure, where permutation-inversion isomers are lumped together. Hence, there are $\mathcal{N}_{\text{min}}$ nodes. Two nodes are connected by an edge if a transition state exists between the corresponding minima. For each N we have obtained $\mathcal{N}_{\text{ts}}$ energetically distinct transition states. Here we need only

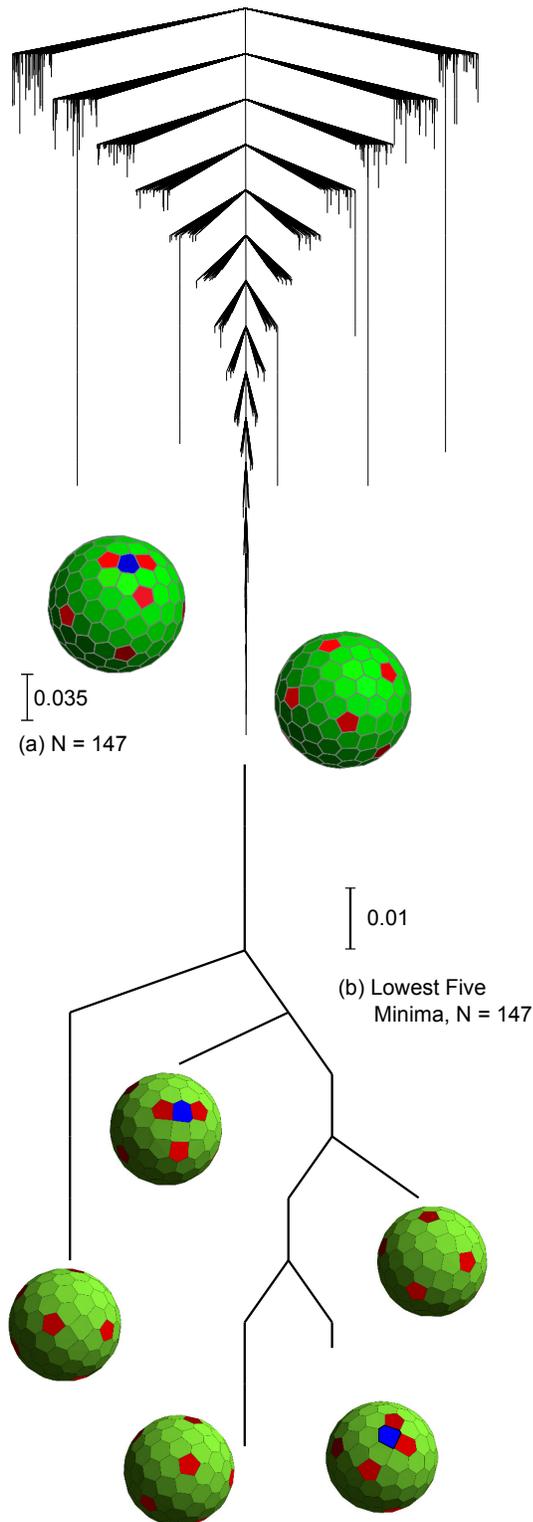Figure 3: Betweenness centrality of the individual minima for $N = 138$.

Figure 2: (a) The disconnectivity graph for $N = 147$. In all cases considered here, the disconnectivity graphs show a typical structure-seeking 'palm tree' organisation. In panel (b) we focus only on the lowest five minima. The insets show the structures of the minimum energy configurations. The pentagons, hexagons, and heptagons indicate that the charges in the centre of the polygons have 5, 6 and 7 neighbours respectively.
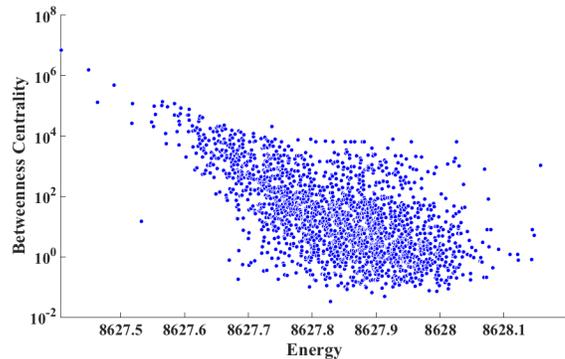
consider whether two minima are connected or not, and

more than one distinct transition state between a pair of minima only counts as a single edge. We call $\mathcal{N}_{\text{edge}}$ the number of edges for the given network, with $\mathcal{N}_{\text{ts}} \geq \mathcal{N}_{\text{edge}}$. As in previous work for Lennard-Jones clusters [74–76], our networks are undirected and unweighted graphs, and hence agnostic about all other information, such as barrier heights or transition rates between the minima.

To further describe our findings, we first define two quantities. The characteristic path length (L) is the average of the shortest path between each pair of nodes in G. We apply an all-pairs shortest path algorithm [77] to the graph G to compute the distance between every two nodes. L is the arithmetic mean of the distances between all pairs of nodes with a finite distance. The local clustering coefficient C_i of the ith node is defined as the fraction of pairs of the neighbouring nodes that are connected over all pairs of the neighbours of the node. The global clustering coefficient C is the average of C_i for $i = 1, \ldots, \mathcal{N}_{\text{min}}$.

A graph is a small-world network if the characteristic path length is similar to, and the clustering coefficient is much higher than, the random graph with the same number of nodes and edges [78]. Small-world properties have been observed in a number of networks of dynamic systems. Our results for the networks of minima of the Thomson Problem for various values of N are reported in Table I. The characteristic path length and the clustering coefficient of the corresponding random graph are denoted as L_0 and C_0, respectively. It is evident that L is as small as L_0, while C is much larger than C_0, and hence the small-world characteristics of the networks are established. The network diameter values, defined in terms of the longest shortest path length, are 5 ($N = 132, 135, 138, 141, 144$), 6 ($N = 147$) and 7 ($N = 150$).

Another important network property is the betweenness centrality, which is defined for each node as the number of shortest paths from all nodes to all others that pass through the node under consideration. Betweenness centrality determines how *central* the node is. In Figure 3, we plot the betweenness centrality of all the nodes of our networks. Our results reveal that the global minimum of the Thomson Problem is always the most central in the network. The number of connections (the node degree) of minima as a function of energy is plotted in Figure 4. The figure clearly shows that low-lying minima are highly connected,

N	$\mathcal{N}_{\text{min}}$	$\mathcal{N}_{\text{ts}}$	$\mathcal{N}_{\text{edge}}$	L	L_0	C	C_0
132	1183	28284	8700	2.3003	2.8959	0.6032	0.0124
135	1585	51832	11285	2.2368	3.0391	0.6932	0.009
138	3226	88999	20150	2.1791	3.4865	0.6312	0.0039
141	4165	100085	38210	2.5684	3.1487	0.5871	0.0044
144	4534	136519	33113	2.3369	3.4445	0.7142	0.0032
147	6644	151299	39241	2.4314	3.8247	0.6375	0.0018
150	9774	178728	87203	2.7601	3.5163	0.4312	0.0018

Table I: Analysis of networks for different values of N. $\mathcal{N}_{\text{min}}$, $\mathcal{N}_{\text{ts}}$ and $\mathcal{N}_{\text{edge}}$ are the number of minima (nodes), energetically distinct transition states, and edges, respectively. L and C are the characteristic path length and the clustering coefficient of each network, while L_0 and C_0 are the characteristic path length and the clustering coefficient of the corresponding random graph.
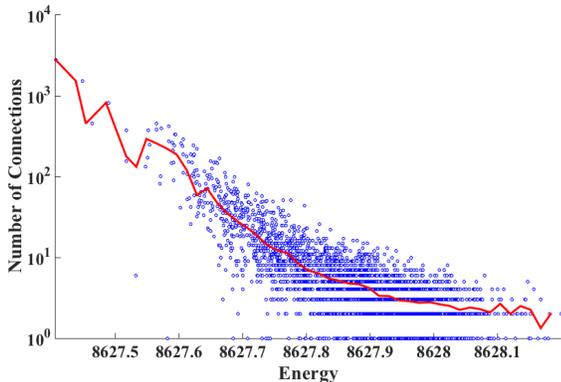

Figure 4: Potential energy minima vs the number of connection at the minimum is plotted, for $N = 138$. The line is the binned average.

making them hubs, unlike the higher energy minima.

DISCUSSION AND CONCLUSION

In this paper we have characterised the potential energy landscape of the Thomson Problem for selected sizes up to $N = 150$. We confirmed that both the number of minima and transition states grow exponentially with N, albeit with a small exponential factor due to the long range nature of the Coulomb interactions. This exponential increase makes the searches for the global minima of the Thomson Problem progressively more difficult. However, by analysing the disconnectivity graphs, we find that for the sizes investigated here, the landscapes exhibit clear structure-seeking organisation. The global minima for systems characterised by such funnelled potential energy landscapes can usually be located easily, even when the total number of minima is large. The asymmetry of the energy barriers makes it easy to escape from high to low energy minima, while the reverse transitions are significantly slower.

We have analysed the networks consisting of local minima and the connections between them defined by transition states, and find that they exhibit small world proper-

ties [78]. Our results provide further evidence to support the conjecture that the small-world phenomenon might be another generic feature of landscapes with the structure-seeking 'palm tree' organisation [79]. Moreover, we found that the low-lying minima are generally significantly more connected than those at higher energy, suggesting scale-free properties. Further statistical tests [80] are required to confirm this behaviour. We note that similar kinetic hubs have been identified for biomolecules in previous work [79, 81, 82]. It is important to note that these networks are static. Hence, the scale-free phenomenon, if confirmed, requires explanation beyond the usual preferential attachment schemes [83].

Our results are relevant for addressing Smale's 7th problem. For the sizes considered here, the global minimum is, on average, only a few transition states $[O(\log \mathcal{N}_{\text{min}})]$ away from any random starting point. $\mathcal{N}_{\text{min}}$ grows exponentially with N, and the increase in the average number of connections is linear. Since the diameter of the networks is typically 5 or 6 (and at most 7), the global minimum is never further than a few steps away, even from the highest-lying minimum. Moreover, the betweenness centrality is largest, by orders of magnitude, for the global minimum, so the majority of shortest paths between all pairs of minima pass through the global minimum, i.e. the global minimum is the central node of these networks. Hence finding the global minimum and exploiting the funnelled/small-world structure of the landscape, is relatively straightforward from a numerical optimisation point of view. Interestingly, though our results suggest that finding the global minimum of the Thomson Problem may be relatively easy, finding an answer to the Smale problem is NP-hard [84]. Constructing and analysing network of minima for the logarithmic version of the potential [17] may provide more concrete details on the mathematics behind Smale's 7th problem.

The present results agree with the observation [74] that funnelled energy landscapes display small world characteristics. In the future we will explore whether these two features are generally correlated, or if a counterexample can be found. Another avenue for future work is to extend our analysis to larger particle numbers. Our previous work on the Thomson Problem [85] found that global minima for for $N > 400$ start to display alternative defect motifs. We expect the potential energy landscape to display multiple funnels in this regime, and it will be interesting to see whether the small world phenomenon found here will be preserved.

In the future, we will further analyse the network properties of this model by including weights and directions for the edges, depending on the barrier heights and kinetic transition rates. We also plan to develop more specific algorithms to locate local and global minima by exploiting small-world properties [86–88]. Analysing the appropriately weighted and directed networks of *free* energy minima [89] and transition states may provide additional insight into the Thomson Problem. Furthermore, invesetigating network properties of higher index saddles may also provide insights to develop novel optimization algorithms [90].

――――――

* dmehta@nd.edu
† jchen16@nd.edu
‡ dchen@nd.edu
§ halim.kusumaatmaja@durham.ac.uk
¶ dw34@cam.ac.uk

[1] J. J. Thomson, The London, Edinburgh, and Dublin Philosophical Magazine and Journal of Science **7**, 237 (1904).
[2] D. L. Caspar and A. Klug, Physical principles in the construction of regular viruses, in *Cold Spring Harbor symposia on quantitative biology*, volume 27, pages 1–24, Cold Spring Harbor Laboratory Press, 1962.
[3] C. J. Marzec and L. A. Day, Biophysical journal **65**, 2559 (1993).
[4] R. F. Bruinsma, W. M. Gelbart, D. Reguera, J. Rudnick, and R. Zandi, Physical review letters **90**, 248101 (2003).
[5] R. Zandi, D. Reguera, R. F. Bruinsma, W. M. Gelbart, and J. Rudnick, PNAS **101**, 15556 (2004).
[6] H. W. Kroto et al., Nature **318**, 162 (1985).
[7] E. J. Davis, Aerosol Science and Technology **26**, 212 (1997).
[8] A. R. Bausch et al., Science **299**, 1716 (2003).
[9] P. Lipowsky, M. J. Bowick, J. H. Meinke, D. R. Nelson, and A. R. Bausch, Nat. Mater. **4**, 407 (2005).
[10] T. Einert, P. Lipowsky, J. Schilling, M. J. Bowick, and A. R. Bausch, Langmuir **21**, 12076 (2005).
[11] H. Kusumaatmaja and D. J. Wales, Phys. Rev. Lett. **110**, 165502 (2013).
[12] G. M. J. Paulose, D. R. Nelson, and V. N. Manoharan, Science **343**, 634 (1904).
[13] W. T. M. Irvine, V. Vitelli, and P. M. Chaikin, Nature **468**, 947 (2010).
[14] W. T. M. Irvine, M. J. Bowick, and P. M. Chaikin, Nat. Mater. **11**, 948 (2012).
[15] E. Bendito, M. J. Bowick, A. Medina, and Z. Yao, Phys. Rev. E **88**, 012405 (2013).
[16] S. Smale, The Mathematical Intelligencer **20**, 7 (1998).
[17] S. Smale, Lecture given on the occasion of Arnold's 60th birthday at the Fields Institute, Toronto. (1997).
[18] Smale's 7th problem rather considers a general form of the potential, r^α, with the spherical constraints. The special values $\alpha = 0$ and 1 correspond to a logarithmic potential and the Thomson problem respectively. In Ref. [17] $\alpha = 0$ is considered as the 'main' problem (and the Thomson problem listed as a special case of the general problem) and more mathematicians are focused on this version of the problem. In Ref. [16], $\alpha = 1$ seems to have (most likely, erroneously) termed as the 'main' problem and is a popular model in chemistry and physics. In the asymptotic limit, both versions of the problems are similar in the following sense: a solution to Thomson problem is known to have an asymptotically optimal logarithmic potential. This statement is proven both ways in Refs. [91, 92]. In any case, both versions of the problem share the same importance and qualitative features. We thank Carlos Beltrán and Edward Saff for clarifying these issues.
[19] To be more precise, a real number algorithm in the sense of [93] is required.
[20] M. Shub and S. Smale, J. Complexity **9**, 4 (1993).
[21] D. Armentano, C. Beltrán, and M. Shub, Transactions of the American Mathematical Society **363**, 2955 (2011).
[22] A. Edelman and E. Kostlan, Bulletin of the American Mathematical Society **32**, 1 (1995).
[23] L. T. Wille, Nature **324**, 46 (1986).
[24] T. Erber and G. M. Hockney, J. Phys. A **24**, L1369 (1991).
[25] E. L. Altschuler, T. J. Williams, E. R. Ratner, F. Dowla, and F. Wooten, Phys. Rev. Lett. **72**, 2671 (1994).
[26] T. Erber and G. M. Hockney, Phys. Rev. Lett. **74**, 1482 (1995).
[27] E. L. Altschuler et al., Phys. Rev. Lett. **78**, 2681 (1997).
[28] T. Erber and G. M. Hockney, Adv. Chem. Phys. **98**, 495 (1997).
[29] J. R. Morris, D. M. Deaven, and K. M. Ho, Phys. Rev. B **53**, R1740 (1996).
[30] E. L. Altschuler and A. Pérez-Garrido, Phys. Rev. E **71**, 047703 (2005).
[31] E. L. Altschuler and A. Perez-Garrido, Phys. Rev. E **73**, 036108 (2006).
[32] D. J. Wales and S. Ulker, Phys. Rev. B **74**, 212101 (2006).
[33] D. J. Wales, H. McKay, and E. L. Altschuler, Phys. Rev. B **79**, 224115 (2009).
[34] J. S. Brauchart, D. P. Hardin, and E. B. Saff, Bulletin of the London Mathematical Society **41**, 621 (2009).
[35] J. Brauchart, D. Hardin, and E. Saff, Contemp. Math **578**, 31 (2012).
[36] M. Bowick, C. Cecka, and A. Middleton, Thomson problem @ s.u., http://physics.syr.edu/condensedmatter/thomson/thomson.htm.
[37] N. N. Andreev, East J. Approx **2**, 459 (1996).
[38] R. E. Schwartz, arXiv preprint arXiv:1001.3702 (2010).
[39] E. B. Saff and A. B. Kuijlaars, The mathematical intelligencer **19**, 5 (1997).
[40] A. Kuijlaars and E. Saff, Transactions of the American Mathematical Society **350**, 523 (1998).
[41] A. Pérez-Garrido and M. A. Moore, Phys. Rev. B **60**, 15628 (1999).
[42] A. M. Livshits and Y. E. Lozovik, Chem. Phys. Lett. **314**, 577 (1999).
[43] M. J. Bowick, D. R. Nelson, and A. Travesset, Phys. Rev. B **62**, 8738 (2000).
[44] M. Bowick, A. Cacciuto, D. R. Nelson, and A. Travesset, Phys. Rev. Lett. **89**, 185502 (2002).
[45] M. J. Bowick, A. Cacciuto, D. R. Nelson, and A. Travesset, Phys. Rev. B **73**, 024115 (2006).
[46] L. Giomi and M. J. Bowick, Phys. Rev. E **78**, 010601 (2008).
[47] T. LaFave Jr, Journal of Electrostatics **72**, 39 (2014).
[48] O. M. Becker and M. Karplus, J. Chem. Phys. **106**, 1495 (1997).
[49] D. J. Wales, M. A. Miller, and T. R. Walsh, Nature **394**, 758 (1998).
[50] J. N. Murrell and K. J. Laidler, Trans. Faraday. Soc. **64**, 371 (1968).
[51] F. Noé and S. Fischer, Curr. Op. Struct. Biol. **18**, 154 (2008).
[52] D. Prada-Gracia, J. Gómez-Gardenes, P. Echenique, and F. Fernando, PLoS Comput. Biol. **5**, e1000415 (2009).
[53] D. J. Wales, Curr. Op. Struct. Biol. **20**, 3 (2010).
[54] D. J. Wales, Gmin: A program for basin-hopping global optimisation, basin-sampling, and parallel tempering, http://www-wales.ch.cam.ac.uk/software.html.
[55] D. J. Wales, Optim: A program for geometry optimisation and pathway calculations, http://www-wales.ch.cam.ac.uk/software.html.
[56] Z. Li and H. A. Scheraga, Proc. Natl. Acad. Sci. USA **84**, 6611 (1987).

[57] D. J. Wales and J. P. K. Doye, J. Phys. Chem. A **101**, 5111 (1997).

[58] D. J. Wales and H. A. Scheraga, Science **285**, 1368 (1999).

[59] D. J. Wales, *Energy Landscapes*, Cambridge University Press, Cambridge, 2003.

[60] J. Nocedal, Mathematics of Computation **35**, 773 (1980).

[61] D. Liu and J. Nocedal, Math. Prog. **45**, 503 (1989).

[62] D. Asenjo, J. D. Stevenson, D. J. Wales, and D. Frenkel, J. Phys. Chem. B **117**, 12717 (2013).

[63] S. A. Trygubenko and D. J. Wales, J. Chem. Phys. **120**, 2082 (2004).

[64] G. Henkelman, B. P. Uberuaga, and H. Jónsson, J. Chem. Phys. **113**, 9901 (2000).

[65] L. J. Munro and D. J. Wales, Phys. Rev. B **59**, 3969 (1999).

[66] Y. Kumeda, L. J. Munro, and D. J. Wales, Chem. Phys. Lett. **341**, 185 (2001).

[67] We compare our results with the estimate on the number of minima, $0.382 \exp(0.0497N)$, as given in [26], the number of minima from a fit to the number of minima found, $(0.31701 \pm 0.1) \exp((0.0518 \pm 0.0012)N)$ and estimated number of minima $\exp(-3.97635 \pm 0.1992) \exp(0.0789298 \pm 0.00176)N)$ (with choosing the '+' sign for both '$\pm$' in our comparison), as given in [68]. We thank the authors of [68] for clarifying their results.

[68] M. Calef, W. Griffiths, and A. Schulz, J. of Stat. Phys. , 1 (2015).

[69] F. H. Stillinger and T. A. Weber, Science **225**, 983 (1984).

[70] D. J. Wales and J. P. K. Doye, J. Chem. Phys. **119**, 12409 (2003).

[71] J. P. K. Doye, D. J. Wales, and R. S. Berry, J. Chem. Phys. **103**, 4234 (1995).

[72] J. P. K. Doye and D. J. Wales, Science **271**, 484 (1996).

[73] J. P. K. Doye and D. J. Wales, J. Chem. Soc., Faraday Trans. **93**, 4233 (1997).

[74] J. P. K. Doye, Phys. Rev. Lett. **88**, 238701 (2002).

[75] J. P. Doye and C. P. Massen, The Journal of chemical physics **122**, 084105 (2005).

[76] C. P. Massen and J. P. Doye, Physical Review E **71**, 046101 (2005).

[77] T. H. Cormen, C. E. Leiserson, R. L. Rivest, and C. Stein, *Introduction to Algorithms*, MIT press, 3rd edition, 2009.

[78] D. J. Watts and S. H. Strogatz, nature **393**, 440 (1998).

[79] J. M. Carr and D. J. Wales, J. Phys. Chem. B **112**, 8760 (2008).

[80] A. Clauset, C. R. Shalizi, and M. E. Newman, SIAM review **51**, 661 (2009).

[81] A. Cavalli, U. Haberthür, E. Paci, and A. Caflisch, Prot. Sci. **12**, 1801 (2003).

[82] D. Gfeller, D. M. de Lachapelle, P. De Los Rios, G. Caldarelli, and F. Rao, Phys. Rev. E **76**, 026113 (2007).

[83] A. L. Barabási and R. Albert, Science **286**, 509 (1999).

[84] C. Beltrán, Constructive Approximation **37**, 135 (2013).

[85] D. J. Wales and S. Ulker, Physical Review B **74**, 212101 (2006).

[86] D. Mehta, T. Chen, J. D. Hauenstein, and D. J. Wales, The Journal of chemical physics **141**, 121104 (2014).

[87] D. Mehta, T. Chen, J. W. Morgan, and D. J. Wales, The Journal of chemical physics **142**, 194113 (2015).

[88] T. Chen and D. Mehta, arXiv preprint arXiv:1504.06622 (2015).

[89] F. Rao and A. Caflisch, Journal of molecular biology **342**, 299 (2004).

[90] C. Hughes, D. Mehta, and D. J. Wales, The Journal of chemical physics **140**, 194104 (2014).

[91] P. Leopardi, Advances in Computational Mathematics , 1 (2013).

[92] C. Beltrán, Foundations of Computational Mathematics **15**, 125 (2015).

[93] L. Blum, F. Cucker, M. Shub, and S. Smale, *Complexity and real computation*, Springer Science & Business Media, 2012.